Front. Med. 2017, 11(3): 410–422
DOI 10.1007/s11684-017-0527-6

RESEARCH ARTICLE

# Annexin A2-S100A10 heterotetramer is upregulated by PML/RARα fusion protein and promotes plasminogen-dependent fibrinolysis and matrix invasion in acute promyelocytic leukemia

Dan Huang[1,*], Yan Yang[1,*], Jian Sun[1,*], Xiaorong Dong[1], Jiao Wang[1], Hongchen Liu[1], Chengquan Lu[2,#], Xueyu Chen[1], Jing Shao (✉)[2,a], Jinsong Yan (✉)[1,b]

[1]*Dalian Key Laboratory of Hematology, Liaoning Hematopoietic Stem Cell Transplantation Medical Center, Department of Hematology of the Second Hospital of Dalian Medical University, Dalian 116027, China;* [2]*Dalian Key Laboratory of Hematology, Liaoning Hematopoietic Stem Cell Transplantation Medical Center, Department of Environmental Health and Toxicology, School of Public Health, Dalian Medical University, Dalian 116044, China*



**Abstract** **Aberrant expression of annexin A2-S100A10 heterotetramer (AIIt) associated with PML/RARα fusion protein causes lethal hyperfibrinolysis in acute promyelocytic leukemia (APL), but the mechanism is unclear. To facilitate the investigation of regulatory association between ANXA2 and promyelocytic leukemia/retinoic acid receptor α (PML/RARα) fusion protein, this work was performed to determine the transcription start site of ANXA2 promoter with rapid amplification of 5′-cDNA ends analysis. Zinc-induced U937/PR9 cells expressed PML/RARα fusion protein, and resultant increases in ANXA2 transcripts and translational expressions of both ANXA2 and S100A10, while S100A10 transcripts remained constitutive. The transactivation of ANXA2 promoter by PML/RARα fusion protein was 3.29 ± 0.13 fold higher than that by control pSG5 vector or wild-type RARα. The overexpression of ANXA2 in U937 transfected with full-length ANXA2 cDNA was associated with increased S100A10 subunit, although S100A10 transcripts remained constitutive. The tPA-dependent initial rate of plasmin generation (IRPG) in zinc-treated U937/PR9 increased by 2.13-fold, and cell invasiveness increased by 27.6%. Antibodies against ANXA2, S100A10, or combination of both all remarkably inhibited the IRPG and invasiveness in U937/PR9 and NB4. Treatment of zinc-induced U937/PR9 or circulating APL blasts with all-trans retinoic acid (ATRA) significantly reduced cell surface ANXA2 and S100A10 and associated reductions in IRPG and invasiveness. Thus, PML/RARα fusion protein transactivated the ANXA2 promoter to upregulate ANXA2 and accumulate S100A10. Increased AIIt promoted IRPG and invasiveness, both of which were partly abolished by antibodies against ANXA2 and S100A10 or by ATRA.**

**Keywords** annexin A2-S100A10 heterotetramer; PML/RARα fusion protein; plasmin; cell invasion; acute promyelocytic leukemia

## Introduction

Acute promyelocytic leukemia (APL) is a distinct subtype of acute myelogenous leukemia and is characterized by a recurrent chromosomal translocation t(15;17)(q22;q21), known as promyelocytic leukemia/retinoic acid receptor α (PML/RARα) fusion gene. The derivative PML/RARα fusion protein drives the leukemogenic processes associated with APL [1]. APL is now curable by treatment with all-trans retinoic acid (ATRA) and/or arsenic trioxide [2]. Indeed, 94.1% to 95% of newly diagnosed APL patients achieve hematological complete remission (HCR), with a five-year relapse-free survival rate of 94.8% [3]. Even in those that do relapse, the five-year event-free survival is 83.3% [4].

Despite high levels of HCR and long-term survival, 3.2% to 7.3% of APL patients still die early mainly due to

Received November 22, 2016; accepted February 8, 2017
Correspondence: [a]jshao@uw.edu; [b]yanjsdmu@126.com

[*]These authors contributed equally to this work.

[#]Current address: Jinzhou City Center for Disease Control and Prevention, Jinzhou 121000, China

severe bleeding diathesis, which is a form of coagulopathy [5]. Furthermore, approximately 2.5% to 4.8% of APL patients experience post-remission relapse of central nervous system leukemia (CNS-L) [6]. Therefore, reducing the incidence of coagulopathy-related early death and preventing CNS-L relapse will ultimately improve outcomes for APL patients. At the time of diagnosis, approximately 80% to 90% of APL patients are suffering from coagulopathy, manifested predominantly as hyperfibrinolysis [7]. Hyperfibrinolysis is mainly triggered by annexin A2-S100A10 heterotetramer (AIIt), which is aberrantly expressed by APL leukemic blasts [8]. AIIt comprises two ANXA2 and two S100A10 (p11) subunits [9]. When anchored at the cell surface, it acts as a receptor for the assembly of plasminogen (PLG) and tissue plasminogen activator (tPA). The resultant PLG/tPA/AIIt complex accelerates (by up to 60-fold) the tPA-dependent conversion of PLG to plasmin [10], which is a factor involved in the degradation of fibrinogen/fibrin and extracellular matrix (ECM) components. Therefore, the aberrant expression of AIIt by APL blasts may lead to plasmin overproduction and subsequent hyperfibrinolysis and ECM degradation; the latter may facilitate cell invasion into extramedullary sites, including central nervous system.

While aberrant expression of either ANXA2 or S100A10 or both is associated with fibrinolysis in APL [11], the underlying mechanism is still unclear. Therefore, this study aimed to uncover the functional significance of aberrant expression of AIIt and clarify the regulatory associations between AIIt and PML/RARα.

## Materials and methods

### Cell lines

U937/PR9, U937/MT, U937, NB4, and COS-7 cells were kindly provided by Professor Xiaodong Xi, Shanghai Institute of Hematology, Shanghai Jiao Tong University School of Medicine, China and maintained in RPMI 1640 or DMEM as described elsewhere [12].

### Isolation of APL blasts

This study has been approved by the Ethics Committee of the Second Hospital of Dalian Medical University. On the basis of informed consents, peripheral blood samples were collected from nine newly diagnosed APL patients treated with oral ATRA (45 mg/d) on day 0 (pre-treatment) and on days 1, 2, 3, and 6. Blood samples were centrifuged with lymphocyte separation medium (TBDscience, China) according to the manufacturer's protocol, and the white cell layers were collected and cultured in RPMI 1640 [13].

### Extraction of RNA and DNA

RNA and DNA were prepared from cells or peripheral blood using extraction kit (9767, 9112, 9450; Takara, Japan) per the manufacturer's protocol.

### Determination of transcription start site of *ANXA2* promoter by rapid amplification of 5′-cDNA ends (5′-RACE)

Thus far, the transcription start site (TSS) of *ANXA2* promoter has not been determined. In the current study, based on the known coding DNA sequence (CDS) of *ANXA2* gene, 3′-primers (outer primer, 5′-CTTGTAGACTCTGTTAATTTCCTG-3′; inner primer, 5′-TACTGAGCAGGTGTCTTCAATAGG-3′) specific for *ANXA2* CDS and designated primers in SMARTer RACE 5′/3′Kit (634859; Takara Bio, Japan) were used for amplifying *ANXA2* fragments by PCR and subsequently nested-PCR reaction according to the manufacturer's manual. The amplified *ANXA2* fragments were analyzed by 1% agarose gel electrophoresis and then purified with TaKaRa MiniBEST Agarose Gel DNA Extraction Kit (9762; Takara, Japan). The extracted *ANXA2* fragments were sequenced with 3′-end inner primer of *ANXA2* for the above-mentioned nested-PCR reaction.

### Plasmid construction

To generate eukaryotic expression plasmids for *ANXA2* and *S100A10*, cDNA was synthesized from total RNA and subjected to PCR using a PrimeScript high fidelity RT-PCR kit (R022A; Takara, Japan) and primers containing recognition sites for *Kpn*I (forward primer) and *Xho*I (reverse primer) restriction endonucleases. The primer sequences were as follows: *ANXA2*, 5′-GC*GGTACC*ATGTCTACTGTTCACGAAATC-3′ and 5′-CG*CTCGAG*TCAGTCATCTCCACCACACA-3′; *S100A10*, 5′-GC*GGTACC*ATGCCATCTCAAATGGA-3′ and 5′-CG*CTCGAG*CTACTTCTTTCCCTTCTG-3′. Full-length *ANXA2* and *S100A10* cDNAs were ligated into the eukaryotic expression vector pcDNA 3.1 (Invitrogen, USA) to yield pcDNA-A2 and pcDNA-S100A10, respectively.

pGL3.1 plasmids containing a luciferase reporter gene driven by our newly identified *ANXA2* promoter (pGL3-A2) or the *S100A10* promoter (pGL3-S100A10) were constructed. In brief, human genomic DNA was used as a PCR template to construct luciferase reporter plasmids. The 5′-flanking region of the putative human *ANXA2* promoter (−567/+ 120 region) or the human *S100A10* gene promoter (−1498/+ 89 region) was amplified using PCR primers containing recognition sites for *Kpn*I and *Xho*I. The primers used to amplify the *ANXA2* and *S100A10* promoters were as follows: *ANXA2*, 5′-GATGGTACCAAAGCGAGTAACAGCA-3′ and 5′-GATCTC-

GAGGTACCCTTCTTCCCA-3′; *S100A10*, 5′-GAGGTACCGAGATTTCCTCCACTGGTGA-3′ and 5′-GACTCGAGCTCACCTTGGCCGAGGC-3′. The PCR fragments corresponding to the truncated promoters were then ligated into the luciferase gene reporter vector, pGL3-Basic (Promega, USA), to yield pGL3-A2 and pGL3-S100A10. All constructed plasmids were verified by DNA sequencing.

The pSG5-RARα, pSG5-PML/RARα, and pRL-SV40 vectors were kindly provided by Professor Xiaodong Xi [14].

**Transfection and luciferase activity assay**

COS-7 cells at $0.5 \times 10^5$ were seeded into a 48-well plate and grown to 80% confluence. Cells (in triplicate wells) were then transiently co-transfected with 150 ng luciferase reporter plasmid (pGL3-A2 or pGL3-S100A10), 150 ng of eukaryotic expression plasmid (pSG5, pSG5-RARα, pSG5-PML/RARα, pcDNA-A2, or pcDNA-S100A10), and 50 ng of pRL-SV40 using Lipofectamine 2000 reagent (11668, Invitrogen, USA), according to the manufacturer's instructions.

The luciferase activity assay was performed 24 h after the transient co-transfections. Co-transfected cells were lysed with passive lysis buffer prior to measurement of firefly and *Renilla* luciferase activity using Dual-Luciferase kit (E1901; Promega, USA) and aluminometer (Berthesda, Germany). All assays were performed in triplicate wells, and each assay was repeated three times.

**Stable sublines**

Twenty micrograms of eukaryotic expression plasmid (pcDNA-A2 or pcDNA-S100A10) was added to $0.8 \times 10^7$ U937 cells resuspended in 800 μl of fetal bovine serum (FBS)-free RPMI 1640 in a 0.4 cm cuvette. The cells were then electroporated at 300 V for 30 ms in single square wave mode using Gene Pulser II system (Bio-Rad, USA). After incubating on ice for 20 min, the cells were cultured in 20 ml of RPMI 1640 medium supplemented with 15% FBS. Stable sublines expressing the ANXA2 or S100A10 proteins were selected using Geneticin (G418; Gibco, USA). These sublines were named U937-A2 and U937-S100A10.

**Real-time quantitative PCR by TaqMan**

TaqMan real-time quantitative PCR (QT-PCR) was performed in a Prism 7500 PCR system (ABI, USA). In brief, first-strand cDNA was synthesized from 100 ng of total RNA and subjected to TaqMan QT-PCR (RR064A; Takara, Japan) to detect the expression of *ANXA2* and *S100A10* mRNA. The house-keeping gene β actin served as the internal control [15]. The following primers were used for QT-PCR: *ANXA2*, F 5′-TGTCTACTGTTCACGAAATCCTGT-3′, R 5′-TCTTCAATAGGCCAAAATCACCGTCT-3′, probe 5′-FAM TGACCAACCGCAGCAATGCACA TAMRA-3′; *S100A10*, F 5′-GCCTCGCCAAGGCTTCA-3′, R 5′-TTATCCCCAGCGAATTTGTG-3′, probe 5′-FAM TGGAACACGCCATGGAAACCATGA TAMRA-3′; β actin, F 5′-GAGCGCGGCTACAGCTT-3′, R 5′-TCCTTAATGTCACGCACGATTT-3′, probe 5′-FAM ACCACCACGGCCGAGCGG TAMRA-3′. The PCR conditions were as follows: initial incubation at 98 °C for 2 min, followed by 40 cycles of denaturation at 98 °C for 10 s, annealing at 60 °C for 15 s, and extension at 68 °C for 30 s. The data (fold changes in the Ct values for each of the genes) were analyzed using the $2^{-\Delta\Delta Ct}$ method. Statistical differences between groups were determined using the Mann–Whitney U test. All tests were two-sided, and a $P$ value of $< 0.05$ was considered significant.

**Cell lysates and nuclear extracts**

To obtain whole-cell lysate, cells were rinsed with phosphate-buffered saline (PBS), lysed in RIPA buffer (20 mmol/L Tris, pH 7.5, 150 mmol/L NaCl, 1 mmol/L EDTA, 1 mmol/L EGTA, 1% Triton X-100, 2.5 mmol/L sodium pyrophosphate, 1 mmol/L β-glycerophosphate, 1 mmol/L $Na_3VO_4$, 1 μg/ml leupeptin, and 1 mmol/L phenylmethylsulfonyl fluoride (PMSF)). The supernatant was collected after centrifugation at $12\,000 \times g$ for 15 min at 4 °C.

Nuclear extracts were obtained with some modifications [16]. All steps were performed at 4 °C. In brief, $1 \times 10^7$ U937/PR9 cells were washed in chilled PBS and then collected by centrifugation. The cell pellet was suspended in 1 ml of ice-cold buffer A (10 mmol/L Hepes pH 7.9, 1.5 mmol/L $MgCl_2$, 10 mmol/L KCl, and 1 mmol/L DTT) containing protease inhibitor cocktail (05892791001, Roche, Germany) and allowed to swell for 10 min. The swelled cell pellet was then incubated with 0.5 ml of buffer A containing NP-40 (0.2%) and 0.5 mmol/L PMSF for 5 min to release the cell nuclei. Following centrifugation at 5000 r/min for 5 min, the nuclear pellet was collected and resuspended in 150 μl of ice-cold buffer B (20 mmol/L Hepes pH 7.9, 0.4 mol/L NaCl, 1 mmol/L EDTA, and 0.5 mmol/L DTT) supplemented with protease inhibitor cocktail and 0.5 mol/L PMSF. The suspension was vortexed for 20 s every 5 min over a period of 30 min and then centrifuged at $10\,000 \times g$ for 20 min. The clear supernatant containing the nuclear extract was then used for Western blotting.

**Flow cytometry analysis**

Cells ($5 \times 10^5$) were rinsed with PBS and incubated with the primary monoclonal antibodies or with pre-immunized

serum at a final concentration of 30 μg/ml for 30 min in the dark at 4 °C. The cells were then washed three times in PBS (cells were centrifuged at 800 × *g* for 3 min between washes) and incubated with an FITC-conjugated goat anti-mouse antibody (1:20) (sc-2010; Santa Cruz, USA) for 30 min at 4 °C. The collected cells were immediately analyzed on a FACS Calibur flow cytometer (BD, USA). The primary monoclonal antibodies against human ANXA2 (directed against tPA binding "tail" domain [amino acids 1–50]) (sc-28385; Santa Cruz, USA) and against human S100A10 (directed against amino acids 2–97) (sc-81153; Santa Cruz, USA) and a mouse pre-immunized antibody (sc-2025; Santa Cruz, USA) were used for flow cytometry as mentioned above [17].

### Western blotting

Anti-ANXA2, -S100A10, -β actin (sc-8432, Santa Cruz, USA), -RARα (sc-551, Santa Cruz, USA), -PML/RARα, and -lamin B (sc-6216, Santa Cruz, USA) antibodies were used to detect corresponding proteins on Western blots.

Protein concentrations were measured using BCA protein assay kit (p1002, Beyotime, China). 60 μg of protein samples were fractionated on 8% SDS-polyacrylamide gels and then transferred to nitrocellulose membranes. The membranes were blocked with 5% nonfat milk in Tris-buffered saline containing 0.1% Tween-20 (TBS-T) and then incubated with primary antibodies at 4 °C for 12 h, followed by a 2 h incubation with horseradish peroxidase-labeled rabbit anti-mouse IgG (sc-358914, Santa Cruz, USA) at a dilution of 1:2000 at room temperature. The blots were then probed with Pierce ECL Western blotting substrate (32106, Thermo, USA) to visualize immunoreactive bands.

### Plasmin generation assay

Cells ($1 \times 10^6$) were suspended in 1 ml incubation buffer (IB) (140 mmol/L NaCl, 4 mmol/L KCl, 10 mmol/L Hepes, 0.2% glucose, 1 mmol/L $MgCl_2$, and 3 mmol/L $CaCl_2$) prior to the addition of mouse monoclonal antibodies against ANXA2 and/or S100A10 or a pre-immunized antibody as a control antibody (all at 60 μg/ml), for 45 min at 4 °C. After washing twice in IB, cells were resuspended in IB containing 170 mmol/L N-terminal glutamic acid PLG from human plasma (191342; MP Bio, USA) for 1 h at 4 °C. Both t-PA (12 nmol/L) (T5451; Sigma, USA) and the fluorogenic plasmin substrate AFC-81 (166 μmol/L) [D-Valine-leucine- lysine-7-amino-4-trifluoromethyl-coumarin] (AFC081, MPBio, USA) were then added. Finally, hydrolysis of the substrate produced by the cells was measured at 2 min intervals at 400 nm (excitation) and 505 nm (emission) in a fluorescence spectrophotometer (F-2700, Hitachi, Japan). Data were expressed as relative fluorescent units (RFU). The initial rate of plasmin generation (IRPG) was calculated by linear regression analysis of plots of RFU versus time squared ($RFU/t^2$) as described previously [18].

### Matrix invasion assay

Transwell inserts (6.5 mm, 8 μm pore size; 3422, Corning, USA) were coated with Matrigel (356230; BD Biosciences, USA), according to the manufacturer's protocol. The Matrigel was diluted to 0.5 mg/ml with cold sterile water and kept on ice. Aliquots (50 μl/insert) of diluted Matrigel were spread over the surface of pre-chilled inserts and allowed to dry overnight. Cells ($4 \times 10^4$/well) were washed three times with PBS and then preincubated with either mouse pre-immune IgG (sc-2025) or monoclonal antibodies against ANXA2 and/or S100A10 (each at 40 μg/ml) at 4 °C for 45 min prior to plating into the transwell inserts. The Matrigel-coated transwell inserts were then placed in a 24-well plate containing RMPI 1640 supplemented with 20% FBS. PLG (1 μg/ml) was then added to the appropriate inserts and the cells incubated at 37 °C for 18 h. The number of cells that migrated across the membrane was counted by two independent observers (five fields per membrane were selected; magnification, 40 ×).

### Statistical analysis

All data on qPCR, Western blot, IRPG, and cell invasion were represented by mean ± SD. All experiments were independently performed three times and each experiment performed in triplicate. Significance on IRPG cell invasion was analyzed using one-way analysis of variance. A $P$ value of $< 0.05$ was considered statistically significant.

## Results

### The increased expression of AIIt is caused by PML/RARα-induced upregulation of ANXA2

High levels of AIIt expression are observed in a variety of cells, including macrophages, endothelial cells, and malignant cells (particularly APL blasts) [19]. First, we separately examined the expression of AIIt subunits, ANXA2 and S100A10, in U937/PR9 cells (promonocytic cells) carrying the PML-RARα coding sequence under the control of a zinc-inducible promoter [20], because the association between aberrant AIIt and PML/RARα is unclear [16].

Fig.1A shows the expression of ANXA2 mRNA transcripts varied at time points in zinc-induced U937/PR9 cells. As observed, the copy numbers of ANXA2 transcripts markedly increased in a time-dependent manner upon exposure to 100 μmol/L zinc. Specifically, with β

actin as the control gene, the level of ANXA2 transcripts started to increase at 2 h (a (17.3 ± 1.58)-fold increase over the constitutive level) and persistently increased to 106.3 ± 0.37 fold at 72 h post exposure. By contrast, S100A10 transcripts maintained only 0.62 ± 0.54 fold to 1.74 ± 0.98 fold with the internal control of gene β actin (Fig. 1B). Analysis by Western blotting on U937/PR9 cell lysates using anti-ANXA2 and anti-S100A10 antibodies showed that the expression of ANXA2 and S100A10 increased 2 h after zinc induction. Moreover, blotting with an anti-RARα antibody confirmed inducible PML/RARα that appeared at 1 h after zinc induction (Fig. 1C). The induction of ANXA2 transcripts and ANXA2 protein promptly followed upon the expression of PML/RARα fusion protein, whereas the increase in S100A10 protein was not in parallel with a constitutive level of S100A10 transcripts during the zinc induction in U937/PR9 cells (Fig. 1A–1C). This observation suggests that the increased expression of S100A10 may be regulated post-translationally rather than post-transcriptionally. In accordance with this finding, flow cytometry analysis demonstrated that the number of cells showing cell surface ANXA2 and S100A10 increased by 26.9% ($P < 0.05$) and 18.9% ($P < 0.05$), respectively, after a 24 h exposure to zinc (Fig. 1D).

To exclude any direct involvement of zinc in

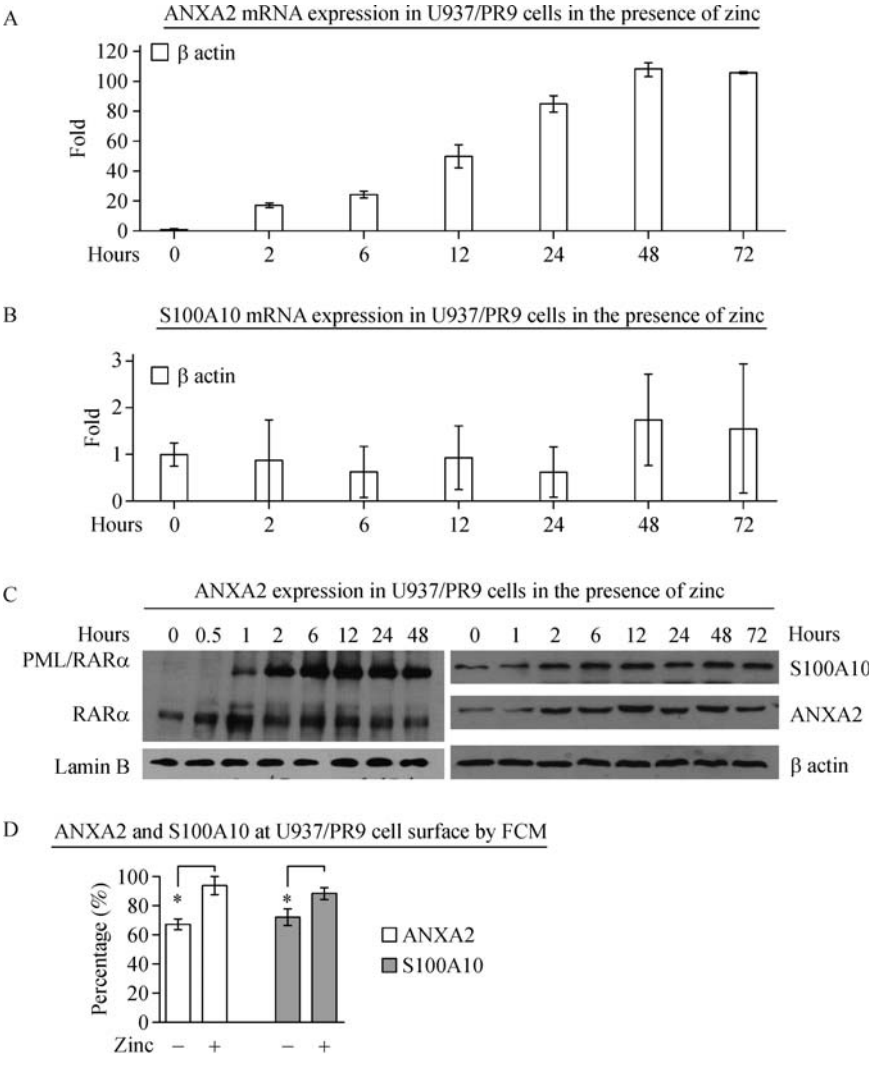


**Fig. 1** PML/RARα fusion protein upregulated AIIt expression. (A) Using house-keeping gene β actin as the internal control, ANXA2 transcripts increased from constitutive level up to 106.3 ± 0.37 fold at 72 h in U937/PR9 cells with induction of 100 μmol/L zinc at varied time points. (B) S100A10 transcripts maintained no more than 1.74 ± 0.98 fold with the internal control gene of β actin at varied time points. (C) U937/PR9 cell nuclear extracts expressed PML/RARα fusion protein with induction of 100 μmol/L zinc, and U937/PR9 cell lysates with anti-ANXA2 and anti-S100A10 antibodies showed that the expression of ANXA2 and S100A10 increased 2 h after zinc induction. (D) By flow cytometry analysis, U937/PR9 cell-surface ANXA2 and S100A10 increased by 26.9% and 18.9%, respectively, after a 24 h exposure to zinc. *$P < 0.05$.

upregulating ANXA2 and S100A10, U937/MT cells were exposed to 100 μmol/L zinc for over 24 h, and the transcripts and protein of AIIt subunits expressed at constant levels (data not shown), suggesting that the upregulation of AIIt in U937/PR9 cells was not the direct effect of zinc. Collectively, these data indicate that ANXA2 was upregulated by zinc-induced PML/RARα protein.

### Determination of the transcription start site

5′-RACE analysis was utilized for localizing the TSS of *ANXA2* promoter with human U937 cells. Based on the known CDS of *ANXA2* gene, one agarose band was obtained from the cDNA amplified using gene-specific primer located in the exon 6 of the *ANXA2* gene. Nucleotide base G located at 60397986 of the genomic sequence NC_000015.10 on chromosome 15 was determined as the TSS of *ANXA2* promoter by DNA sequencing of the extracted PCR band (Fig. 2).

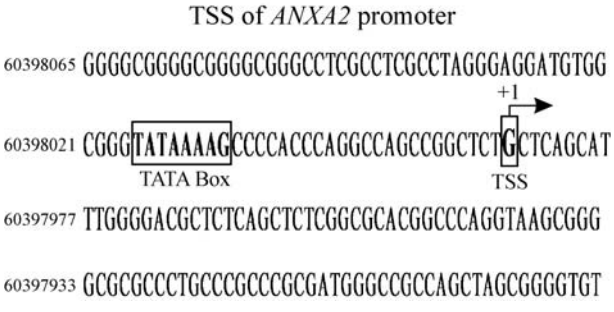


**Fig. 2** Determination of transcription start site of *ANXA2* promoter by 5′-RACE. The 3′-primers (outer primer, 5′-CTTGTAGACTCTGTTAATTTCCTG-3′; inner primer, 5′-TACTGAGCAGGTGTCTTCAATAGG-3′) specific for *ANXA2* CDS and designated primers in SMARTer RACE 5′/3′Kit (634859; Takara Bio, Japan) were used to amplify *ANXA2* fragments by PCR, followed by a nested-PCR reaction. The amplified *ANXA2* fragments were resolved on a 1% agarose gel and purified with TaKaRa MiniBEST Agarose Gel DNA Extraction Kit (9762; Takara, Japan). The extracted *ANXA2* fragments were sequenced with 3′-end inner primer of *ANXA2*, and nucleotide base **G**, which is located at 60397986 of the genomic sequence NC_000015.10 on chromosome 15, was determined as the TSS of *ANXA2* promoter.

### Overexpression of ANXA2 increases the expression of S100A10

Given that ANXA2 and S100A10 jointly constitute the AIIt complex, the increased expression of one may facilitate the expression of the other. Thus, U937 cells were electroporated with pcDNA-A2 or pcDNA-S100A10 to induce the overexpression of ANXA2 or S100A10, respectively. U937-A2 cells showed the overexpression of ANXA2 mRNA and protein, and similarly U937-S100A10 cells overexpressed S100A10 mRNA and protein. However, U937-A2 sublines also showed an increased expression in S100A10 protein, though with a constitutive expression of S100A10 mRNA (Fig. 3A and 3B). This observation indicates that the overexpression of ANXA2 can lead to increased expression of S100A10 via post-translational regulation.

### PML/RARα transactivates the *ANXA2* promoter

To examine whether PML/RARα regulates the transcription of *ANXA2* and *S100A10*, the pSG5-PML/RARα and pSG5-RARα expression plasmids or the pSG5 vector were co-transfected into COS-7 cells along with the pGL3-A2 or pGL3-S100A10 reporters, which contain fragments of the *ANXA2* and *S100A10* promoters located upstream of the firefly luciferase gene.

The luciferase activity assay showed that the transactivation of pSG5-PML/RARα on pGL3-A2 promoter increased by $3.29 \pm 0.13$ fold compared with pSG5 vector, whereas the transactivation of pSG5-RARα on pGL3-A2 only resulted in a $(1.24 \pm 0.03)$-fold increase (Fig. 3C). However, no effect was observed on the pGL3-S100A10 promoter (Fig. 3D), indicating that the transactivation of pGL3-A2 was specific to PML/RARα. In addition, after co-transfection for 24 h, COS-7 cells were exposed to $10^{-6}$ mol/L ATRA, and a marked reduction in the luciferase activity to a constitutive activity was detected in cells transfected with pSG5-PML/RARα ($1.12 \pm 0.08$ fold), while no difference in pSG5-RARα-transfected COS-7 cells was observed (Fig. 3C and 3D). The data indicate that ATRA treatment can effectively abolish the increase in ANXA2 promoter-mediated luciferase activity, which was transactivated by PML/RARα fusion protein.

The AIIt-mediated increases in IRPG and invasiveness of zinc-induced U937/PR9 and NB4 cells were abrogated by monoclonal antibodies against ANXA2 and/or S100A10.

AIIt plays a critical role in tPA-dependent plasminogen activation, which is a process inclined to be predominantly mediated by the S100A10 subunit [21]. Hence, monoclonal antibodies that block PLG binding sites were used to examine the rate of plasmin generation at the cell surface. When U937/PR9 cells were treated with fluorogenic plasmin substrate AFC-81 and tPA, fluorogenic assay showed a 2.13-fold increase (from $1.75 \pm 0.84$ RFU/min$^2$ to $3.73 \pm 1.67$ RFU/min$^2$) in the IRPG in the presence of zinc at 24 h (Fig. 4A). However, the IRPG in zinc-induced U937/MT cells was similar to that in U937/MT cells ($1.9 \pm 0.3$ versus $2.0 \pm 0.5$ RFU/min$^2$) in the absence of zinc (data were not shown), suggesting that the zinc-induced expression of PML/RARα, but not zinc itself, was

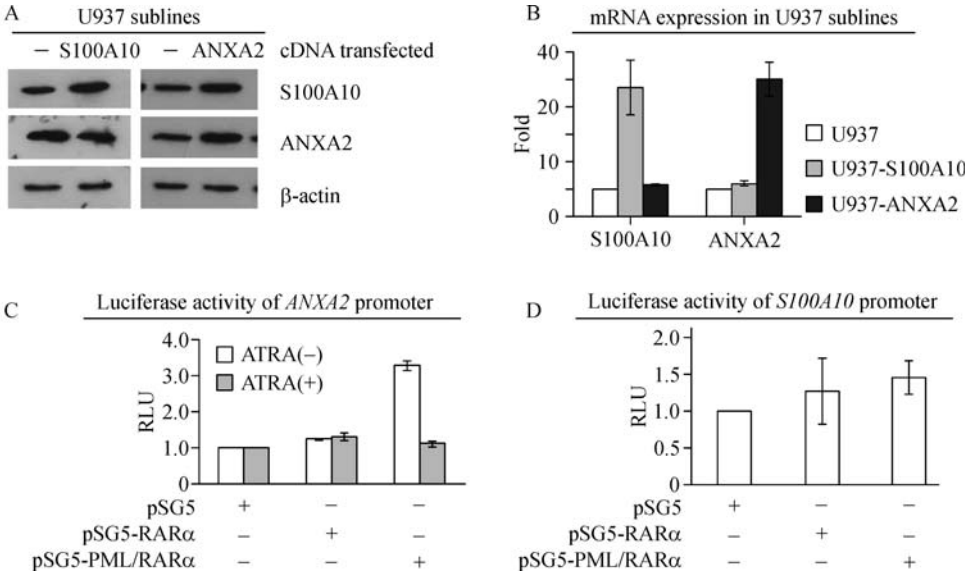


**Fig. 3** PML/RARα fusion protein transactivated *ANXA2* promoter to upregulate *ANXA2*, which led to the increases of S100A10 subunit. (A) U937 cells transfected with ANXA2 cDNA overexpressed ANXA2 and S100A10 with Western blotting; however, U937 transfected with S100A10 cDNA showed an overexpression of S100A10 but no effect on ANXA2 subunit. (B) U937 cells transfected with S100A10 cDNA or ANXA2 cDNA showed an elevated expression of S100A10 or ANXA2 transcripts, respectively. (C) Eukaryocytic expression plasmids, including pSG5-PML/RARα, pSG5-RARα, or pSG5 vector, and pRL-SV40 vector, along with pGL3-A2 promoter reporter or pGL3-S100A10 promoter reporter, were co-transfected into COS-7 cells; luciferase activity showed that pSG5-PML/RARα plasmid led to a markedly elevated luciferase activity, which was abolished by 24-h exposure of $10^{-6}$ mol/L ATRA. (D) No transactivated luciferase activity occurred on S100A10 promoter by pSG5-PML/RARα, pSG5-RARα plasmid.

responsible for the increased plasminogen activation. The addition of monoclonal antibodies against ANXA2 or S100A10, or a combination of both, markedly inhibited the increase in the IRPG in zinc-induced U937/PR9 cells compared with that in U937/PR9 cells ($P < 0.05$).

Enhanced plasminogen activation leads to increased ECM degradation [22]; therefore, we further examined cell invasiveness in the presence of antibodies against the two AIIt subunits in PML/RARα-harboring cells. The invasiveness of zinc-treated U937/PR9 cells was 27.6% greater than that of controls without addition of zinc (60.29% ± 0.71% vs. 87.13% ± 1.11%) (Fig. 4B). Blockage with antibodies against ANXA2 or S100A10, or a combination of both, markedly inhibited the invasion of zinc-treated U937/PR9 cells.

Similar effects were observed in NB4 cells. As shown in Fig. 4C and 4D, the IRPG was inhibited in the presence of monoclonal antibodies against ANXA2 or S100A10, or a combination of both, and the invasiveness of NB4 cells was also inhibited in the presence of above-mentioned antibodies.

## ATRA downregulates AIIt expression in cells harboring PML/RARα

ATRA rapidly alleviates severe bleeding diathesis in APL patients and is predominantly associated with aberrant expression of AIIt [12]. Therefore, PML/RARα-harboring cells were then treated with $10^{-6}$ mol/L ATRA, and the expression and the plasminogen activation of AIIt were examined. As shown in Fig. 5A, ATRA caused a reduction in the expression of ANXA2 and S100A10 in zinc-induced U937/PR9 cells, beginning at 48 h post-treatment. The cell surface expression of AIIt subunits also decreased following ATRA treatment (Fig. 5B). Specifically, flow cytometry showed that the proportion of cells showing cell surface expression of ANXA2 was 93.9% ± 6.2% prior to ATRA treatment but dropped to 33.4% ± 1.3% at 48 h and 17.2% ± 4.2% at 120 h post-treatment. The proportion of cells expressing S100A10 was 88.3% ± 5.7% prior to ATRA treatment and dropped to 43.8% ± 2.3% at 48 h and 14.9% ± 2.7% at 120 h post-treatment. As shown in Fig. 5C and 5D, ANXA2 transcripts showed reduction at 12 h after ATRA treatment with β actin as the internal control, whereas S100A10 transcripts showed a decreased expression at 24 h, indicating that ATRA was responsible for decreased ANXA2 and S100A10 proteins.

Consistent with the downregulation of AIIt upon exposure to ATRA, the IRPG in zinc-induced U937/PR9 cells decreased to 0.57 ± 0.04 RFU/min$^2$ at 96 h post-ATRA from initial 2.18 ± 0.47 RFU/min$^2$ prior to ATRA treatment (Fig. 5E). Meanwhile, the invasiveness of zinc-induced U937/PR9 cells decreased to 13.18% ± 8.38% at 96 h after exposure to ATRA from initial 82.84% ± 6.99%

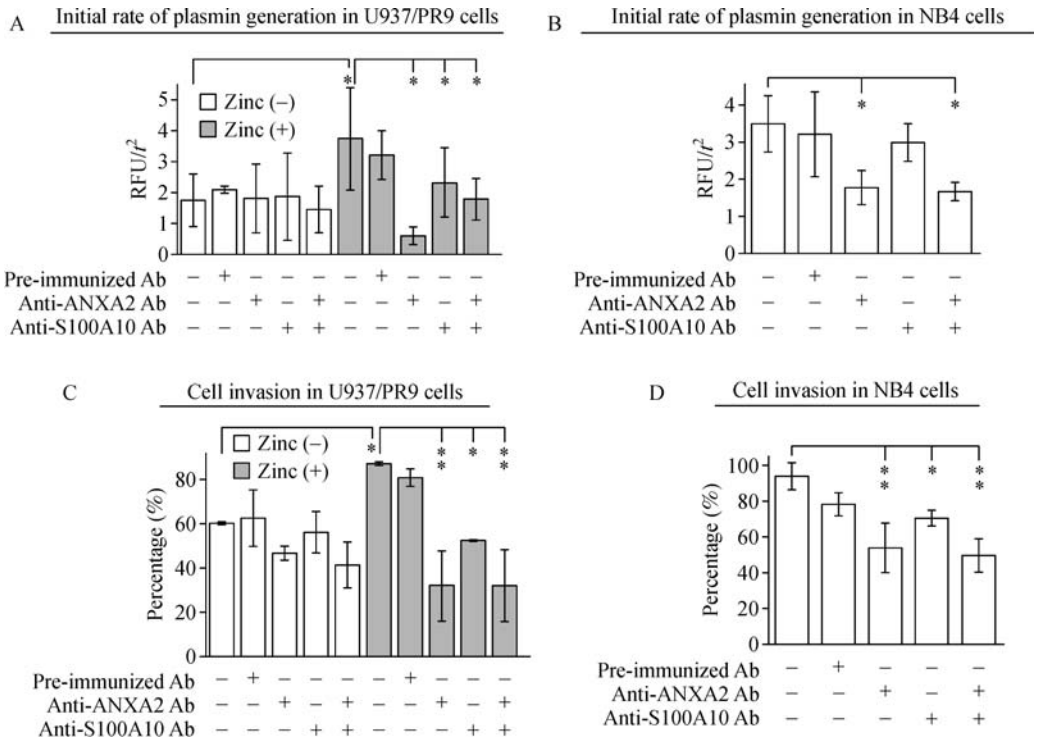


**Fig. 4** AIIt promoted initial rate of plasmin generation (IRPG) and invasiveness in zinc-induced U937/PR9 and NB4 cells, which were abrogated by monoclonal antibodies against ANXA2 and/or S100A10. (A) U937/PR9 cells showed an increase in IRPG from 1.75 ± 0.84 RFU/min$^2$ to 3.73 ± 1.67 RFU/min$^2$ in the presence of zinc at 24 h, when addition of monoclonal antibodies against ANXA2 or S100A10, or a combination of both, markedly inhibited the increase of the IRPG in zinc-induced U937/PR9 cells compared with that in U937/PR9 cells (*$P < 0.05$). (B) Cell invasion in zinc-treated U937/PR9 cells increased to 87.13% ± 1.11% from 60.29% ± 0.71% in U937/PR9 cells without zinc induction. Blockage with antibodies against ANXA2 or S100A10, or a combination of both, markedly inhibited the invasion of zinc-treated U937/PR9 cells (*$P < 0.05$). (C) IRPG in NB4 cells was 3.49 ± 0.77 RFU/min$^2$ and was inhibited in the presence of monoclonal antibodies against ANXA2 or S100A10, or a combination of both (*$P < 0.05$, **$P < 0.01$). (D) Cell invasion was 93.62% ± 7.62% in NB4 cells and was inhibited in the presence of monoclonal antibodies against ANXA2 or S100A10, or a combination of both (*$P < 0.05$, **$P < 0.01$).

(Fig. 5F). The data demonstrated that the downregulation of AIIt by ATRA treatment led to the reduction of IRPG and cell invading ability in zinc-induced U937/PR9 cells.

The above-mentioned observations were also tested in ATRA-treated NB4 cells, and the IRPG started to decrease to 2.38 ± 1.08 RFU/min$^2$ at 24 h and 1.83 ± 0.90 RFU/min$^2$ at 96 h after exposure to ATRA from initial 3.95 ± 0.41 RFU/min$^2$ prior to ATRA treatment (Fig. 5G). Accordingly, the invasiveness of NB4 cells decreased from 74.55% ± 19.37% prior to ATRA treatment to 8.26% ± 5.26% at 96 h post-ATRA treatment (Fig. 5H).

Overall, these data suggest that ATRA inhibits both plasminogen activation and the invasiveness of leukemia cells by downregulating AIIt.

## ATRA treatment reduces the IRPG and cell invasion in APL blasts isolated from patients

The expression and functional significance of AIIt were further investigated in blasts isolated from nine newly diagnosed APL patients undergoing induction therapy with ATRA from January 2015 to October 2016. Along with oral ATRA treatment, the peripheral mononuclear cells were isolated for follow-up testing.

Along with the ATRA treatment, both ANXA2 transcripts and S100A10 transcripts from all patients presented a decreased trend, with β actin as the internal control. In details, ANXA2 transcripts decreased from onefold at pre-treatment to 0.35 ± 0.19 fold at day 6 post-treatment of ATRA (Fig. 6A) and S100A10 transcripts from onefold at pre-treatment to 0.38 ± 0.12 fold at day 6 post-ATRA (Fig. 6B).

Flow cytometry analysis on cell surface expression of ANXA2 or S100A10 revealed a similar downward trend to their respective transcripts throughout the treatment course (Fig. 6C and 6D). For example, ANXA2 expression decreased from 15.80% ± 4.81% at pre-treatment to 3.74% ± 1.49% at day 6 post-ATRA and S100A10 expression from 27.9% ± 8.7% at pre-treatment to 2.94% ± 1.41% at day 6 post-ATRA.

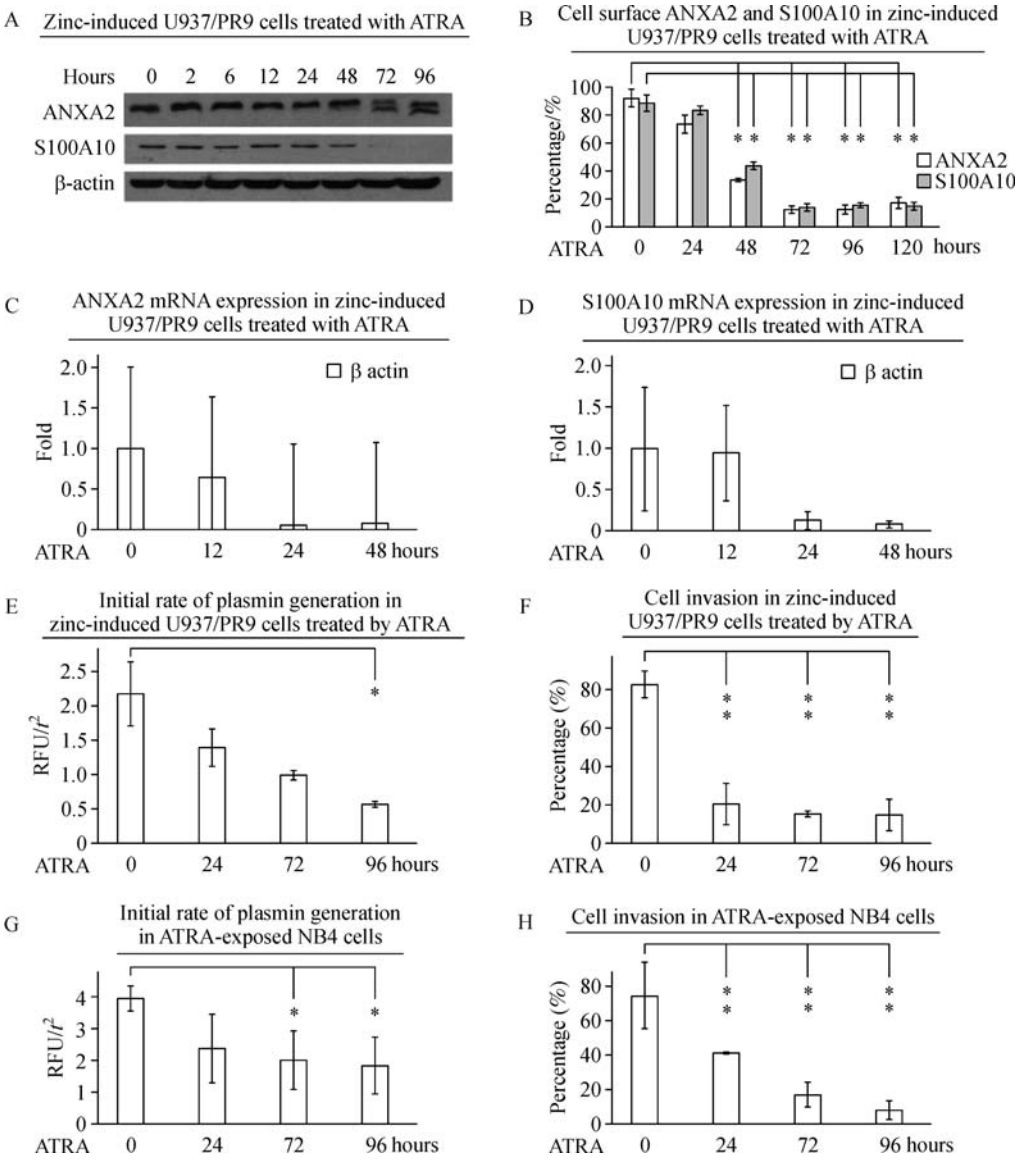


**Fig. 5** ATRA downregulated the AIIt expression in cells harboring PML/RARα and subsequently led to the reduction of initial rate of plasmin generation (IRPG) and cell invasion. (A) ATRA reduced the expression of ANXA2 and S100A10 in zinc-induced U937/PR9 cells after exposure to $10^{-6}$ mol/L ATRA. (B) Cell surface expression of AIIt subunits decreased following ATRA treatment. As revealed by flow cytometry, the expression of ANXA2 at cell surface was 93.9% ± 6.2% prior to ATRA treatment and then dropped to 33.4% ± 1.3% at 48 h and 17.2% ± 4.2% at 120 h post-treatment. The expression of S100A10 was 88.3% ± 5.7% prior to ATRA treatment and dropped to 43.8% ± 2.3% at 48 h and 14.9% ± 2.7% at 120 h post-treatment. $^{**}P < 0.01$. (C) ANXA2 transcripts decreased after ATRA treatment by TaqMan PCR with house-keeping gene β actin as the internal control. (D) S100A10 transcripts showed a decreased expression with β actin as the internal control at varied time points. (E) After exposure to ATRA, the IRPG in zinc-induced U937/PR9 cells decreased to 0.57 ± 0.04 RFU/min$^2$ at 96 h post-ATRA from 2.18 ± 0.47 RFU/min$^2$ prior to ATRA. $^{*}P < 0.05$. (F) After exposure to ATRA, the cell invasion of zinc-induced U937/PR9 cells decreased to 13.18% ± 8.38% at 96 h after exposure to ATRA from 82.84% ± 6.99% before treatment with ATRA. $^{**}P < 0.01$. (G) After exposure to ATRA, the IRPG in NB4 cells started to decrease to 2.38 ± 1.08 RFU/min$^2$ at 24 h and 1.83 ± 0.90 RFU/min$^2$ at 96 h from 3.95 ± 0.41 RFU/min$^2$ prior to ATRA. $^{*}P < 0.05$. (H) The cell invasion in NB4 cells decreased from 74.55% ± 19.37% pre-treatment of ATRA to 8.26% ± 5.26% at 96 h post-ATRA treatment. $^{**}P < 0.01$.

IRPG was assessed in the isolated APL blasts from nine patients. As shown in Fig. 6E, prior to ATRA treatment, the level of IRPG was measured as 1.66 ± 0.38 fold, whereas the IRPG was reduced to 1.08 ± 0.50 fold at day 3 and 0.33 ± 0.26 fold at day 6 post-ATRA treatment. Also in Fig. 6E, the effect of blockage with antibodies

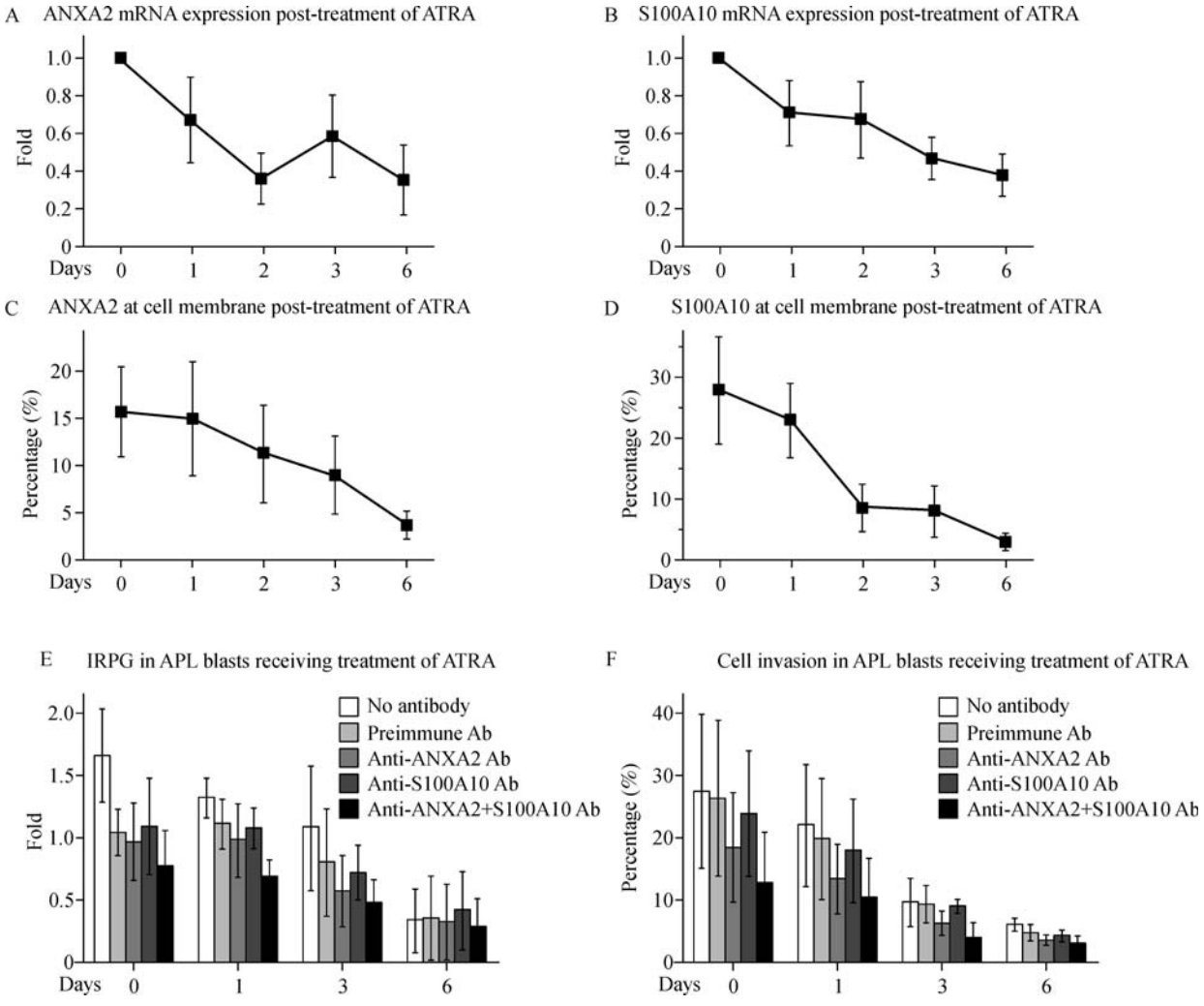


**Fig. 6** Effects of ATRA treatment on the mRNA levels of ANXA2 and S100A10, the cell surface expression of ANXA2 and S100A10, and the IRPG and the cell invasiveness in the isolated APL blasts. The APL blasts were isolated from nine patients newly diagnosed with APL. (A) ATRA treatment decreased ANXA2 transcripts from onefold at pre-treatment to 0.35 ± 0.19 fold at day 6 post-treatment, with β actin as the internal control. (B) ATRA treatment decreased S100A10 transcripts from onefold at pre-treatment to 0.38 ± 0.12 fold at day 6 post-treatment, with β actin as the internal control. (C) Flow cytometry analysis on cell surface expression of ANXA2 expression. ANXA2 expression reduced from 15.80% ± 4.81% prior to treatment to 3.74% ± 1.49% at day 6 post-ATRA treatment. (D) Flow cytometry analysis on cell surface expression of S100A10 expression. S100A10 expression decreased from 27.9% ± 8.7% prior to treatment to 2.94% ± 1.41% at day 6 post-treatment. (E) ATRA treatment decreased the level of IRPG from the pre-treatment level of 1.66 ± 0.38 fold to 1.08 ± 0.50 fold at day 3 and 0.33 ± 0.26 fold at day 6 post-treatment. In addition, blockage with antibodies against ANXA2 or S100A10, or a combination of both, further reduced the IRPG level of the isolated APL blasts from days 1 to 3. However, no inhibitory effect from antibodies was observed at day 6. (F) ATRA treatment decreased the level of the invasiveness of the isolated APL blasts from 27.9% ± 8.70% prior to treatment to 8.08% ± 4.28% at day 3 and 2.95% ± 1.41% at day 6. Antibodies against ANXA2 or S100A10, or a combination of both, further inhibited the invasiveness. However, the inhibitory effects became weaker along with ATRA treatment, particularly at day 6.

against ANXA2 or S100A10, or a combination of both, on the IRPG of the isolated APL blasts was presented. In detail, prior to ATRA treatment (i.e., day 0), antibodies against ANXA2 or S100A10, or a combination of both, all decreased the IRPG in the isolated APL blasts. Along with ATRA treatment, blockage with these antibodies continued to inhibit the IRPG from days 1 to 3. However, no inhibitory effect from antibodies was observed at day 6, suggesting that the cell surface expression of AIIt was markedly downregulated to undetectable levels and thus had no effect on tPA-dependent plasminogen activation.

The invasiveness of the isolated APL blasts was also evaluated. As demonstrated in Fig. 6F, throughout the

ATRA treatment, the invasiveness of the isolated APL blasts decreased from 27.9% ± 8.70% prior to treatment to 8.08% ± 4.28% at day 3 and 2.95% ± 1.41% at day 6. When antibodies against ANXA2 or S100A10, or a combination of both, were used to block the AIIt subunits at the APL cell surface prior to ATRA (i.e., day 0), invasiveness was markedly inhibited. Along with treatment of ATRA, the inhibitory effects notably became weaker, particularly at day 6, indicating that a little AIIt on cell surface remained after ATRA treatment (Fig. 6F).

## Discussion

Although the outcome for most APL patients is optimistic, early death and CNS-L relapse are two major obstacles to an ultimate cure for all. The overproduction of plasmin, which is mediated by aberrant expression of the AIIt complex on APL blasts, is the main cause of hyperfibrinolysis and ECM degradation [23].

APL blasts and NB4 cells express high levels of AIIt, but the reason behind this remains unclear [24]. A study published in 2011 suggests that expression of PML/RARα leads to a remarkable increase in the expression of ANXA2 and S100A10 but only at the translational level [16]. However, the findings from the present study suggest that PML/RARα transcriptionally and post-transcriptionally regulates ANAX2 expression but only translationally regulates S100A10 expression in zinc-induced U937/PR9 cells.

As the transcription start site (TSS) of *ANXA2* promoter has remained undetermined, the present study was the first to localize the TSS by 5-RACE analysis, which would facilitate further investigation of the regulatory association between ANXA2 mRNA and PML/RARα. In addition, ANXA2 plays a key role in regulating the proteolytic activity of plasmin, oncogenesis, and invasion and metastasis of cancer cells [25], then localizing the TSS of *ANXA2* promoter will benefit the research on regulation of ANXA2 expression [26,27]. Thereafter, Cos-7 cells transiently transfected with pSG5-PML/RARα and the promoter-truncated pGL3-A2 or pGL3-S100A10 plasmid revealed remarkable transactivation of the *ANXA2* promoter but not of the *S100A10* promoter, confirming that PML/RARα plays a role in the transcriptional upregulation of ANXA2 mRNA expression.

Simultaneous upregulation of both ANXA2 and S100A10 proteins was also observed, suggesting that a regulatory relationship may exist between ANXA2 and S100A10. Stable U937-A2 sublines showing overexpression of both ANXA2 protein and ANXA2 mRNA expressed constitutive levels of S100A10 mRNA, but higher levels of S100A10 protein indicating S100A10 expression is driven by the overexpression of ANXA2 protein. The association between ANXA2 and S100A10 has been studied both *in vitro* and *in vivo* in the absence of PML/RARα [28]. For example, the levels of S100A10 mRNA and protein in ANXA2( –/– ) L5178Y tumor cells are significantly lower than those in ANXA2( +/+ ) L5178Y cells; indeed, cardiac microvascular endothelial cells obtained from ANXA2 $^{-/-}$ mice show very low levels of S100A10 expression, indicating that lower levels of ANXA2 may cause reduced expression levels of S100A10. Furthermore, N-terminally acetylated ANXA2 binds S100A10 to form the ANXA2-S100A10 complex [29], which protects unpartnered S100A10 from proteasome-dependent degradation [30,31]. Therefore, PML/RARα-driven upregulation of ANXA2 in APL blasts, NB4 cells, and zinc-induced U937/PR9 cells may lead to the post-translational accumulation of S100A10 by protecting it from polyubiquitination and subsequent degradation. AIIt complex increases fibrinolysis and cell invasion through the overproduction of plasmin [28]. The functional significance of PML/RARα-induced incremental increases in AIIt complex expression in APL is unclear. In this study, U937/PR9 cells were used to examine the functional significance of AIIt, a downstream target of the PML/RARα fusion protein. IRPG was 2.13-fold higher and cell invasion 27.6% higher in zinc-induced U937/PR9 cells than in non-induced cells. When zinc-induced U937/PR9 cells were treated with monoclonal antibodies against ANXA2, S100A10, or both to block plasminogen binding sites, IRPG was abolished and cell invasion was reduced; however, all three antibody combinations had a similar effect, suggesting that the expression of PML/RARα in zinc-induced U937/PR9 cells increased the IRPG and cell invasion, both of which are plasminogen-dependent via the AIIt complex.

Although the AIIt complex serves as an assembly site for tPA and PLG, the exact binding sites for tPA and PLG are in a dispute. One hypothesis suggests that lysine residues at the carboxyl-terminal of S100A10 interact with the lysine binding "kringle" domains on tPA and PLG thereby facilitating PLG binding and activation at the cell surface [25]. However, another hypothesis suggests that N-terminal amino acids (1–15) of ANXA2 act as a binding site for tPA and PLG [25], while a third suggests that both ANXA2 and S100A10 harbor exposed lysine residues that are accessible to the "kringle" domains of tPA and PLG [32]. The antibodies used in the present study had a similar effect on the rate of plasmin generation, suggesting that they block the tPA and PLG binding to the AIIt complex to a similar extent. If the binding sites for tPA and PLG are localized at the N-terminal lysine residues of ANXA2 or at the C-terminal lysine residues of S100A10 or at all of these lysines, the antibodies would inhibit the IRPG to differing extents. The antibodies against ANAX2 in combination with S100A10 should have shown a much greater inhibitory effect. The similar inhibitory effects shown by

the two antibodies suggest that the conformation of AIIt may play a critical role in the binding of blocking antibodies. If the theory that the binding site for tPA and PLG resides within the lysine residues at the C terminus of S100A10 was true and that the AIIt complex is formed by binding of the C-terminal region of S100A10 to the N-terminal region of ANXA2 [33], we propose that the structural conformation of the AIIt complex provides a three-dimensional architecture that is recognized by tPA and PLG. When an anti-ANXA2 antibody binds to amino acids 1–15 of ANXA2, it blocks access by tPA and PLG to the C terminus of S100A10. Therefore, although an antibody against ANAX2 may not directly block the binding of tPA and PLG to S100A10, it still blocks the access (via steric hindrance); this may be the reason why all three antibodies showed similar effects on the IRPG and cell invasion.

Most studies examining the function of AIIt either overexpressed or knocked down one of its subunits [34]; however, we used antibodies to examine the pathophysiological function of AIIt while retaining the expression of ANXA2 and S100A10. Results showed that antibodies against either ANXA2 or S100A10 can inhibit the IRPG, suggesting that the AIIt complex may be a potential therapeutic target, and that antibodies targeting the subunits of this complex may reduce the incidence of early death from bleeding diathesis and CNS-L relapse in APL.

ATRA rapidly alleviates severe bleeding diathesis in APL, and earlier administration of ATRA may decrease the early death rate of newly diagnosed APL patients [12]; thus, we examined the role of ATRA in downregulating the expression of AIIt in PML/RARα-harboring cells. The expression level of ANXA2 protein in U937/PR9, NB4, and APL blasts was reduced upon treatment with ATRA, in accordance with their decreases in the IRPG, suggesting that ATRA reduced plasminogen activation by down-regulating the expression of ANXA2. Clinically, bleeding diathesis in APL patients is rapidly alleviated after one week of receiving ATRA therapy [12]. The present study proposed that for newly diagnosed APL patients receiving ATRA, antibodies can be used to reduce the IRPG and further reduce bleeding diathesis during the first week of ATRA treatment; thus, early deaths due to bleeding diathesis may be minimized.

Overall, the data from the present study suggest that PML/RARα directly upregulates ANXA2 expression at the transcriptional level and indirectly upregulates the expression of S100A10. A higher expression of the AIIt complex is consistent with a higher IRPG, which can be abrogated (at least in part) by treatment with antibodies against ANXA2 or S100A10, or by treatment with ATRA. Such antibodies may be a useful therapy for newly diagnosed APL patients.

## Acknowledgements

The authors would like to thank Dr. Xiaodong Xi, Shanghai Institute of Hematology, Shanghai Jiao Tong University School of Medicine, China, for generously providing technical assistance. This work was supported by the National Natural Science Foundation of China (No. 81270606/H0812 to Jinsong Yan; No. 81273031/H2601 to Jing Shao); the Reformation Project in the Key Clinical Departments of Provincial Hospitals on Construction of Diagnosis and Treatment Capacity in Liaoning Province (No. LNCCC-A02-2015 to Jinsong Yan); and the startup funding from Dalian Medical University under Talent Introduction Program (No. 201069 to Jing Shao).

## Compliance with ethics guidelines

Dan Huang, Yan Yang, Jian Sun, Xiaorong Dong, Jiao Wang, Hongchen Liu, Chengquan Lu, Xueyu Chen, Jing Shao, and Jinsong Yan declare that they have no conflict of interest. All procedures followed were in accordance with the ethical standards of the responsible committee on human experimentation (institutional and national) and with the *Helsinki Declaration* of 1975, as revised in 2000 (5). Informed consent was obtained from all patients for being included in the study.

## References

1. Melnick A, Licht JD. Deconstructing a disease: RARα, its fusion partners, and their roles in the pathogenesis of acute promyelocytic leukemia. Blood 1999; 93(10): 3167–3215
2. Hu J, Liu YF, Wu CF, Xu F, Shen ZX, Zhu YM, Li JM, Tang W, Zhao WL, Wu W, Sun HP, Chen QS, Chen B, Zhou GB, Zelent A, Waxman S, Wang ZY, Chen SJ, Chen Z. Long-term efficacy and safety of all-trans retinoic acid/arsenic trioxide-based therapy in newly diagnosed acute promyelocytic leukemia. Proc Natl Acad Sci USA 2009; 106(9): 3342–3347
3. Iland HJ, Bradstock K, Supple SG, Catalano A, Collins M, Hertzberg M, Browett P, Grigg A, Firkin F, Hugman A, Reynolds J, Di Iulio J, Tiley C, Taylor K, Filshie R, Seldon M, Taper J, Szer J, Moore J, Bashford J, Seymour JF; Australasian Leukaemia and Lymphoma Group. All-trans-retinoic acid, idarubicin, and IV arsenic trioxide as initial therapy in acute promyelocytic leukemia (APML4). Blood 2012; 120(8): 1570–1580
4. Iland H, Bradstock K, Seymour J, Hertzberg M, Grigg A, Taylor K, Catalano J, Cannell P, Horvath N, Deveridge S, Browett P, Brighton T, Chong L, Springall F, Ayling J, Catalano A, Supple S, Collins M, Di Iulio J, Reynolds J; Australasian Leukaemia and Lymphoma Group. Results of the APML3 trial incorporating all-trans-retinoic acid and idarubicin in both induction and consolidation as initial therapy for patients with acute promyelocytic leukemia. Haematologica 2012; 97(2): 227–234
5. Zhou J, Zhang Y, Li J, Li X, Hou J, Zhao Y, Liu X, Han X, Hu L, Wang S, Zhao Y, Zhang Y, Fan S, Lv C, Li L, Zhu L. Single-agent arsenic trioxide in the treatment of children with newly diagnosed acute promyelocytic leukemia. Blood 2010; 115(9): 1697–1702
6. Thirugnanam R, George B, Chendamarai E, Lakshmi KM,

Balasubramanian P, Viswabandya A, Srivastava A, Chandy M, Mathews V. Comparison of clinical outcomes of patients with relapsed acute promyelocytic leukemia induced with arsenic trioxide and consolidated with either an autologous stem cell transplant or an arsenic trioxide-based regimen. Biol Blood Marrow Transplant 2009; 15(11): 1479–1484

7. Park JH, Qiao B, Panageas KS, Schymura MJ, Jurcic JG, Rosenblat TL, Altman JK, Douer D, Rowe JM, Tallman MS. Early death rate in acute promyelocytic leukemia remains high despite all-trans retinoic acid. Blood 2011; 118(5): 1248–1254
8. Shen ZX, Shi ZZ, Fang J, Gu BW, Li JM, Zhu YM, Shi JY, Zheng PZ, Yan H, Liu YF, Chen Y, Shen Y, Wu W, Tang W, Waxman S, de Th Hé, Wang ZY, Chen SJ, Chen Z. All-trans retinoic acid/$As_2O_3$ combination yields a high quality remission and survival in newly diagnosed acute promyelocytic leukemia. Proc Natl Acad Sci USA 2004; 101(15): 5328–5335
9. Mathews V, George B, Chendamarai E, Lakshmi KM, Desire S, Balasubramanian P, Viswabandya A, Thirugnanam R, Abraham A, Shaji RV, Srivastava A, Chandy M. Single-agent arsenic trioxide in the treatment of newly diagnosed acute promyelocytic leukemia: long-term follow-up data. J Clin Oncol 2010; 28(24): 3866–3871
10. Liu YJ, Wu DP, Liang JY, Qiu HY, Jin ZM, Tang XW, Fu CC, Ma X. Long-term survey of outcome in acute promyelocytic leukemia: a single center experience in 340 patients. Med Oncol 2011; 28(Suppl 1): S513–S521
11. Avvisati G, Lo Coco F, Mandelli F. Acute promyelocytic leukemia: clinical and morphologic features and prognostic factors. Semin Hematol 2001; 38(1): 4–12
12. Breen KA, Grimwade D, Hunt BJ. The pathogenesis and management of the coagulopathy of acute promyelocytic leukaemia. Br J Haematol 2012; 156(1): 24–36
13. Menell JS, Cesarman GM, Jacovina AT, McLaughlin MA, Lev EA, Hajjar KA. Annexin II and bleeding in acute promyelocytic leukemia. N Engl J Med 1999; 340(13): 994–1004
14. Yan J, Wang K, Dong L, Liu H, Chen W, Xi W, Ding Q, Kieffer N, Caen JP, Chen S, Chen Z, Xi X. PML/RARα fusion protein transactivates the tissue factor promoter through a GAGC-containing element without direct DNA association. Proc Natl Acad Sci USA 2010; 107(8): 3716–3721
15. Flood EC, Hajjar KA. The annexin A2 system and vascular homeostasis. Vascul Pharmacol 2011; 54(3–6): 59–67
16. O'Connell PA, Madureira PA, Berman JN, Liwski RS, Waisman DM. Regulation of S100A10 by the PML-RAR-α oncoprotein. Blood 2011; 117(15): 4095–4105
17. Udalova IA, Kwiatkowski D. Interaction of AP-1 with a cluster of NF-κB binding elements in the human TNF promoter region. Biochem Biophys Res Commun 2001; 289(1): 25–33
18. Meng YS, Khoury H, Dick JE, Minden MD. Oncogenic potential of the transcription factor LYL1 in acute myeloblastic leukemia. Leukemia 2005; 19(11): 1941–1947
19. Dignam JD, Lebovitz RM, Roeder RG. Accurate transcription initiation by RNA polymerase II in a soluble extract from isolated mammalian nuclei. Nucleic Acids Res 1983; 11(5): 1475–1489
20. Surette AP, Madureira PA, Phipps KD, Miller VA, Svenningsson P, Waisman DM. Regulation of fibrinolysis by S100A10 *in vivo*. Blood 2011; 118(11): 3172–3181
21. Brownstein C, Deora AB, Jacovina AT, Weintraub R, Gertler M, Khan KM, Falcone DJ, Hajjar KA. Annexin II mediates plasminogen-dependent matrix invasion by human monocytes: enhanced expression by macrophages. Blood 2004; 103(1): 317–324
22. Kassam G, Choi KS, Ghuman J, Kang HM, Fitzpatrick SL, Zackson T, Zackson S, Toba M, Shinomiya A, Waisman DM. The role of annexin II tetramer in the activation of plasminogen. J Biol Chem 1998; 273(8): 4790–4799
23. Olwill SA, McGlynn H, Gilmore WS, Alexander HD. Annexin II cell surface and mRNA expression in human acute myeloid leukaemia cell lines. Thromb Res 2005; 115(1–2): 109–114
24. Nervi C, Ferrara FF, Fanelli M, Rippo MR, Tomassini B, Ferrucci PF, Ruthardt M, Gelmetti V, Gambacorti-Passerini C, Diverio D, Grignani F, Pelicci PG, Testi R. Caspases mediate retinoic acid-induced degradation of the acute promyelocytic leukemia PML/RARα fusion protein. Blood 1998; 92(7): 2244–2251
25. Bharadwaj A, Bydoun M, Holloway R, Waisman D. Annexin A2 heterotetramer: structure and function. Int J Mol Sci 2013; 14(3): 6259–6305
26. Moreau K, Ghislat G, Hochfeld W, Renna M, Zavodszky E, Runwal G, Puri C, Lee S, Siddiqi F, Menzies FM, Ravikumar B, Rubinsztein DC. Transcriptional regulation of Annexin A2 promotes starvation-induced autophagy. Nat Commun 2015; 6: 8045
27. Huang B, Deora AB, He KL, Chen K, Sui G, Jacovina AT, Almeida D, Hong P, Burgman P, Hajjar KA. Hypoxia-inducible factor-1 drives annexin A2 system-mediated perivascular fibrin clearance in oxygen-induced retinopathy in mice. Blood 2011; 118(10): 2918–2929
28. Madureira PA, Surette AP, Phipps KD, Taboski MAS, Miller VA, Waisman DM. The role of the annexin A2 heterotetramer in vascular fibrinolysis. Blood 2011; 118(18): 4789–4797
29. Sharma MC, Sharma M. The role of annexin II in angiogenesis and tumor progression: a potential therapeutic target. Curr Pharm Des 2007; 13(35): 3568–3575
30. Hou Y, Yang L, Mou M, Hou Y, Zhang A, Pan N, Qiang R, Wei L, Zhang N. Annexin A2 regulates the levels of plasmin, S100A10 and Fascin in L5178Y cells. Cancer Invest 2008; 26(8): 809–815
31. He KL, Deora AB, Xiong H, Ling Q, Weksler BB, Niesvizky R, Hajjar KA. Endothelial cell annexin A2 regulates polyubiquitination and degradation of its binding partner S100A10/p11. J Biol Chem 2008; 283(28): 19192–19200
32. Nazmi AR, Ozorowski G, Pejic M, Whitelegge JP, Gerke V, Luecke H. N-terminal acetylation of annexin A2 is required for S100A10 binding. Biol Chem 2012; 393(10): 1141–1150
33. Hedhli N, Falcone DJ, Huang B, Cesarman-Maus G, Kraemer R, Zhai H, Tsirka SE, Santambrogio L, Hajjar KA. The annexin A2/S100A10 system in health and disease: emerging paradigms. J Biomed Biotechnol 2012; 2012: 406273
34. Das R, Burke T, Plow EF. Histone H2B as a functionally important plasminogen receptor on macrophages. Blood 2007; 110(10): 3763–3772